

Cocaine Self-Administration and Extinction Leads to Reduced Glial Fibrillary Acidic Protein Expression and Morphometric Features of Astrocytes in the Nucleus Accumbens Core

Michael D. Scofield, Hao Li, Benjamin M. Siemsen, Kati L. Healey, Phuong K. Tran, Nicholas Woronoff, Heather A. Boger, Peter W. Kalivas, and Kathryn J. Reissner

ABSTRACT

BACKGROUND: As a more detailed picture of nervous system function emerges, diversity of astrocyte function becomes more widely appreciated. While it has been shown that cocaine experience impairs astroglial glutamate uptake and release in the nucleus accumbens (NAc), few studies have explored effects of self-administration on the structure and physiology of astrocytes. We investigated the effects of extinction from daily cocaine self-administration on astrocyte characteristics including glial fibrillary acidic protein (GFAP) expression, surface area, volume, and colocalization with a synaptic marker.

METHODS: Cocaine or saline self-administration and extinction were paired with GFAP Westerns, immunohistochemistry, and fluorescent imaging of NAc core astrocytes (30 saline-administering and 36 cocaine-administering male Sprague Dawley rats were employed). Imaging was performed using a membrane-tagged lymphocyte protein tyrosine kinase-green fluorescent protein (Lck-GFP) driven by the GFAP promoter, coupled with synapsin I immunohistochemistry.

RESULTS: GFAP expression was significantly reduced in the NAc core following cocaine self-administration and extinction. Similarly, we observed an overall smaller surface area and volume of astrocytes, as well as reduced colocalization with synapsin I, in cocaine-administering animals. Cocaine-mediated reductions in synaptic contact were reversed by the β -lactam antibiotic ceftriaxone.

CONCLUSIONS: Multiple lines of investigation indicate that NAc core astrocytes exist in a hyporeactive state following cocaine self-administration and extinction. Decreased association with synaptic elements may be particularly meaningful, as cessation of chronic cocaine use is associated with changes in synaptic strength and resistance to the induction of synaptic plasticity. We hypothesize that the reduced synaptic colocalization of astrocytes represents an important maladaptive cellular response to cocaine and the mechanisms underlying relapse vulnerability.

Keywords: Astrocyte, Cocaine, Colocalization, GFAP, Nucleus accumbens, Self-administration

<http://dx.doi.org/10.1016/j.biopsych.2015.12.022>

Astrocytes are critically involved in a wide range of physiological processes in the nervous system, including synapse formation, synaptic transmission, neuronal energy metabolism, extracellular ion homeostasis, blood flow, and sleep (1–3). In addition, disruption in astrocyte-mediated modulation of neuronal function has been implicated in a wide range of disease processes, including schizophrenia, depression, and addiction (4). Supporting a role for astrocytes in plasticity associated with drug seeking, Bull *et al.* (5) have shown that activating Gq-coupled signaling via designer receptors exclusively activated by designer drugs (DREADD) receptors selectively expressed in nucleus accumbens (NAc) core astrocytes inhibits motivation to seek ethanol. Similarly, activating glial Gq-DREADD receptors in the NAc core decreases cued

cocaine seeking, an effect mediated by group II metabotropic glutamate receptors (6). In agreement with the proposed role for astrocytes in addiction-related processes, Turner *et al.* (7) reported that transgenic overexpression of a dominant negative component of vesicular release machinery in astrocytes leads to deficits in cocaine reinstatement and conditioned place preference. Collectively, these and other studies support a role for astrocytes in the cellular mechanisms of addiction [for review, see (8)].

A seminal feature of cocaine-induced adaptations in astrocytes is decreased expression and activity of the high-affinity glial glutamate transporter (GLT-1) (9). In general, decreased expression of GLT-1 is associated with an increase in reactive astrogliosis following injury, ischemia, and neural degeneration

(10–12), raising the hypothesis that NAC astrocytes may exist in a state of reactive astrogliosis following self-administration and extinction. Indeed, astrocyte activation has been reported following noncontingent administration of cocaine, methamphetamine, and opiates (13–16) and is associated with methamphetamine-induced neurotoxicity and opiate-induced hypersensitivity to pain (17,18). Further, astrocyte activation is generally characterized by increased expression of the intermediate filament protein, glial fibrillary acidic protein (GFAP) (19). Thus, we hypothesized that operant cocaine self-administration and extinction would similarly impact GFAP expression as well as structural aspects of astrocyte physiology.

However, results from a series of complementary approaches indicated opposite effects of cocaine self-administration. Cocaine self-administration and extinction training rendered NAC astrocytes in a state characterized by decreased GFAP expression, surface area, volume, and decreased colocalization with synapsin I. The cocaine-mediated decrease in synaptic colocalization was reversed by administration of ceftriaxone, a compound previously shown to restore expression of GLT-1, normalize extrasynaptic glutamate levels, and impair cocaine reinstatement (9,20). These data expand the spectrum of the adaptations that occur in response to chronic cocaine exposure in the central nervous system and infer broad implications toward a more complete understanding of the cocaine-induced adaptations in synaptic communication and plasticity responsible for relapse vulnerability.

METHODS AND MATERIALS

Animals and Surgical Procedures

Male Sprague Dawley rats (200–250 g) were purchased from both Harlan (Boston, MA) and Charles River (Indianapolis, IN). They were housed individually in a temperature-controlled environment on a 12-hour reverse light cycle. Following approximately 1 week of environmental acclimation, animals were anesthetized with ketamine (100 mg/kg) and xylazine (7 mg/kg), together with ketorolac analgesic (0.28–0.32 mg/kg). A 13-cm Bio-sil Silastic catheter (0.02 inner diameter, 0.047 outer diameter [Dow Corning, Midland, MI]) was implanted into the right jugular vein, exiting the back attached to a 22-gauge cannula (Plastics One, Wallingford, CT). Prophylactic antibiotic (Timentin 10 mg/0.1 mL, intravenous; GlaxoSmithKline, Research Triangle Park, NC) was administered during surgery and 4 days postoperatively. Catheters were flushed daily with heparin (0.1 mL, 100 U/mL) until the end of self-administration.

For imaging of green fluorescent protein (GFP)-labeled astrocytes, lymphocyte protein tyrosine kinase (Lck)-GFP expressed under the control of the GfaABC1D promoter in adeno-associated virus type 5 (21) was microinjected immediately following catheterization into the nucleus accumbens (1.0 μ L per side, 7.3×10^{12} particles/mL at 0.1 μ L/min) followed by a >15-minute diffusion time, and microinjectors were slowly removed over a period of 1 to 2 minutes. Virus was microinjected into the NAC core with 26-gauge injectors at a 6° angle at the following coordinate (mm): +1.5 anterior/posterior, +2.6 medial/lateral, –7.2 dorsal/ventral (22). Lck

plasmid provided by Baljit Khakh (University of California, Los Angeles) was packaged into adeno-associated virus type 5 by the University of North Carolina at Chapel Hill Viral Vector core.

Behavioral Training

All operant training (2 hours/session) was performed in standard rat modular test chambers (Med Associates, St. Albans, VT) at the same time daily. Before onset of cocaine self-administration, animals received a food training session (10 to 12 hours) in which an active lever press resulted in the administration of a single 45 mg food pellet (Bio-Serv, Flemington, NJ). Following food training, animals were maintained on ~20 g chow per day. Self-administration of cocaine was performed on a fixed-ratio 1 schedule, 0.2 mg per infusion paired with a light and tone (70–72 dB). Each infusion was followed by a 20-second time-out period. Infusions were capped to 40 for the first 2 days of self-administration and unrestricted thereafter. Criteria for self-administration was 10 days of at least 10 cocaine infusions received, followed by 14 to 16 sessions of extinction training. Cocaine was provided by the National Institute on Drug Abuse Drug Supply Program. Ceftriaxone (100 mg/kg, intraperitoneal) (Hospira Worldwide, Inc., Lake Forest, IL) or vehicle (sterile saline) was administered 30 minutes before the last 10 extinction sessions.

Western Blotting and Immunohistochemistry

For Western blotting, animals were rapidly decapitated 24 hours after the last extinction training session. Tissue was homogenized in 0.32 mol/L sucrose, 10 mmol/L 4-(2-hydroxyethyl)-1-piperazineethanesulfonic acid (pH 7.4) and protease/phosphatase inhibitor cocktail (Thermo Scientific, Waltham MA). Following centrifugation at 1000 g for 10 minutes, the supernatant was separated into a crude membrane fraction and a crude cytosolic fraction by centrifugation at 12,000 g for 20 minutes. Protein content in the S2 cytosolic fraction was determined by the bicinchoninic acid method (Thermo Scientific) and 10 μ g was separated on BisTris gels (Bio-Rad, Hercules, CA) and transferred to polyvinylidene fluoride membranes, then probed using anti-GFAP (ab7779, 1:1000; Abcam, Cambridge, MA) and anti-glyceraldehyde 3-phosphate dehydrogenase (1:2000; Cell Signaling, Danvers, MA).

For GFAP immunohistochemistry, animals were deeply anesthetized with pentobarbital 24 hours after the last extinction session and perfused with 150 mL 1 \times phosphate buffer (PB) followed by 200 mL 4% paraformaldehyde in 1 \times PB. Brains were postfixed overnight in 4% paraformaldehyde in 1 \times PB. Brains were then transferred to 30% sucrose in 1 \times PB containing 0.1% sodium azide for 1 to 2 days at 4°C, then transferred to 1 \times phosphate buffered saline (PBS) and sliced 45 μ m on a cryostat. Serial sections (every six sections, approximately 2.6 to 1.0 mm anterior to bregma) were stained for GFAP and visualized using vasoactive intestinal peptide peroxidase substrate as follows: slices were blocked with 10% normal goat serum (NGS) in PBS with Tween (PBST) for an hour and probed at room temperature overnight in anti-GFAP (ab7779, 1:1000; Abcam) in PBST containing 3% NGS. Slices were washed three times (10 minutes each) in PBST containing 3% NGS and

incubated for 1 hour at room temperature in biotinylated goat anti-rabbit (1:200; Vector Labs, Burlingame, CA) in PBST + 3% NGS. Sections were then washed twice in PBST + 3% NGS and once in PBS. Slices were incubated at room temperature with avidin-biotin complex (Vector Labs) and washed three times in PBS before developed in vasoactive intestinal peptide for 15 seconds (SK-4600; Vector Labs). Slices were washed again in PBS three times (10 minutes each) followed by 3×10 -minute wash in PB. Slices were mounted in PB on clean slides (Fisherbrand Superfrost Plus; Fisher, Pittsburgh, PA) and dried and dehydrated in ethanol, and coverslips were added using Permount (Fisher).

Stereological Cell Counts

Quantitative estimates of the total number of GFAP immunoreactive (GFAP-ir) neurons in the NAc core were achieved using an unbiased, stereological cell counting method (23,24). Briefly, the optical fractionator system consists of a computer-assisted image analysis system including a Nikon Eclipse E-600 microscope hard-coupled to a Prior H128 computer controlled x-y-z motorized stage, an Olympus-750 video camera system, a Micron Pentium III 450 computer, and stereological software (Stereoinvestigator; MicroBrightField Inc., Colchester, VT). The NAc core was outlined under low magnification ($10\times$) on every sixth section through the rostrocaudal extent of the NAc core, and the outlined region was measured with a systematic random design of dissector counting frames ($100 \times 100 \mu\text{m}$). Actual mounted section thickness was found to be 35 to $37 \mu\text{m}$, and a $2\text{-}\mu\text{m}$ guard zone was set for the top and bottom of each section. A $40\times$ objective lens with a 1.4 numerical aperture was used to count cells within the counting frames. The selection of the first section from the NAc core in the rostral position was random and every sixth section was counted, rendering a systematic random design. The total number of GFAP-ir neurons was calculated. Outline contours drawn for NAc core cell counts included areas containing GFAP-ir cells and excluded the anterior commissure.

Astrocyte Imaging and Colocalization

For fluorescence imaging and colocalization studies, animals were deeply anesthetized with pentobarbital (100 mg/kg) and perfused with 200 mL PB followed by 200 mL 4% paraformaldehyde in $1\times$ PB. Brains were postfixed for 2 to 5 hours, then transferred to $1\times$ PBS at 4°C . Coronal slices of accumbens ($100 \mu\text{m}$) were prepared on a vibratome and washed three times for 5 minutes in $1\times$ PBS with 2% Triton-X 100 (Fisher), then blocked with 2% NGS in $1\times$ PBS containing 2% Triton-X 100 for 1 hour. Sections were then incubated in 2% NGS-PBST with a rabbit polyclonal antibody against synapsin-1 (Ab8, 1:500; Abcam) overnight at 4°C . Sections were washed three times for 5 minutes in $1\times$ PBST followed by 8 hours at room temperature with an Alexa-594 conjugated goat anti-rabbit antibody (1:1000; Life Technologies, Carlsbad, CA), then washed three more times before slide mounting with ProLong Diamond Antifade (Life Technologies).

Z-stacks were acquired using a Leica laser-scanning confocal microscope SP6 spinning disc confocal (Leica, Buffalo Grove, IL) equipped with the argon (Ar 488 nm), krypton (Kr

568 nm), and helium-neon (He-Ne 633 nm) laser line. GFP was excited using the 488 nm wavelength with a fluorescein filter set, and Alexa 594 labeled synapsin was acquired using the 568 nm wavelength and rhodamine-like filter set. All images were acquired using a $63\times$ oil immersion objective with a $1\times$ digital zoom factor. Acquisition settings were as follows: 1024×1024 frame size, 12-bit image resolution, frame average of 4, and a $2\text{-}\mu\text{m}$ step size. Z-stacks were typically in the range of 22 to $35 \mu\text{m}$. Care was taken to ensure that selected astrocytes were complete through the x, y, and z planes and nonoverlapping (Supplemental Figure S2). Acquired z-stacks were exported to BitPlane Autoquant deconvolution software (10 iterations) (BitPlane, Zurich, Switzerland) (25). Colocalization analysis was performed with BitPlane Imaris three-dimensional (3-D) image analysis software following deconvolution. Lck-GFP images were taken only if viral transduction occurred inside the nucleus accumbens core (22).

Deconvolved 3-D z-stacks were analyzed with Imaris software using the colocalization module. All images were cropped before analysis to reduce file size and to isolate single cells. For background correction, GFP and Alexa 594 signal thresholds were set empirically for each image using the two-dimensional scatter plot of the colocalization module (ImarisColoc). Following manual threshold setting, thresholding, each slice of the 3-D z-stack was manually checked to ensure accurate determination of colocalization. Thresholded signal intensity/total signal intensity was calculated for each channel. We also recorded the percentage of the dataset colocalized (normalized % colocalization relative to the total number of voxels). Imaging and analysis of astrocytes were performed in an unbiased manner, blind to the groups.

Statistical Analyses

Data were analyzed using two-tailed *t* tests when analyzing two groups (cocaine vs. saline) or one-way analysis of variance followed by Bonferroni corrected multiple comparisons when analyzing three groups (cocaine, saline, and cocaine + ceftriaxone).

RESULTS

GFAP Expression Is Reduced in the NAc Core Following Cocaine Self-Administration and Extinction

Western blot analysis revealed a significant reduction in GFAP protein levels in the NAc core following cocaine self-administration and extinction when compared with yoked saline control animals ($t_{14} = 2.967$, $p = .01$; Figure 1B). In contrast, no difference was observed in the dorsomedial prefrontal cortex, including prelimbic and anteriorcingulate regions ($t_{14} = .533$, $p = .60$; Figure 1B). The number of GFAP positive cells was independently assessed using stereology in samples immunohistochemically stained for GFAP following saline or cocaine exposure. In agreement with decreased GFAP protein expression, the number of GFAP-positive gray matter astrocytes in the NAc core was significantly reduced following cocaine self-administration and extinction ($t_{17} = 2.554$, $p = .02$; Figure 1C, D).

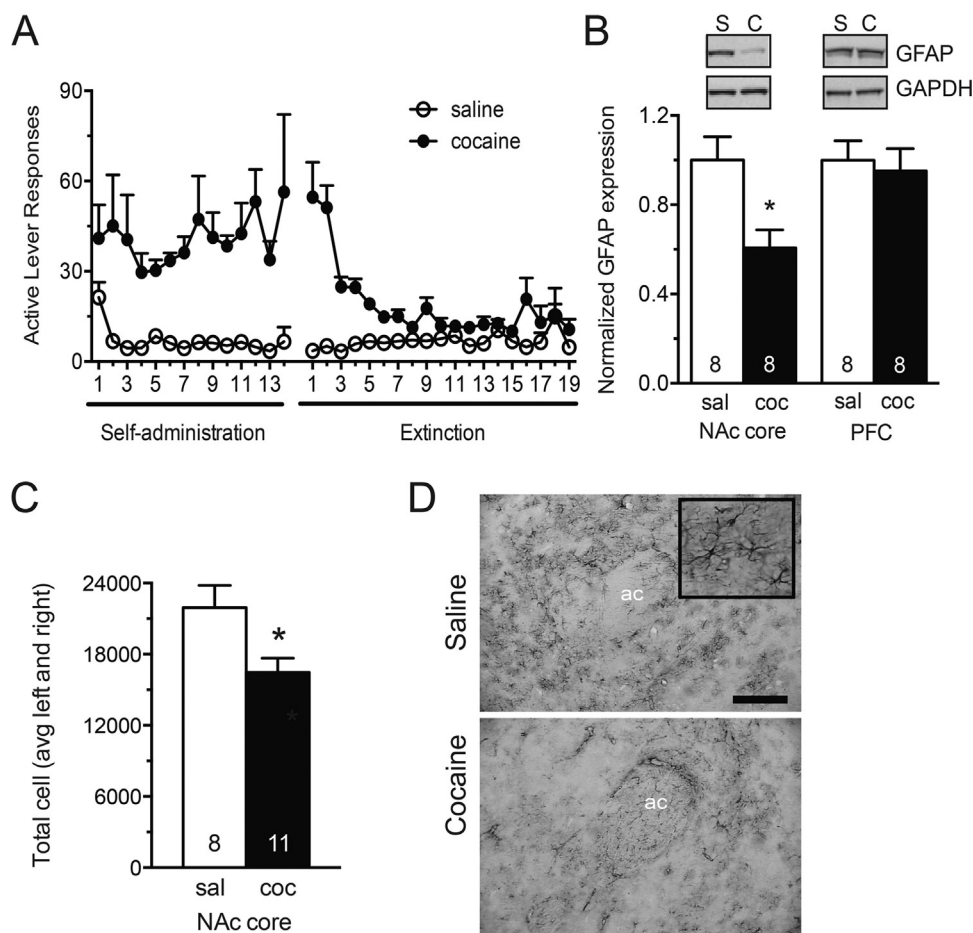


Figure 1. Glial fibrillary acidic protein (GFAP) expression is reduced in nucleus accumbens (NAc) core astrocytes following cocaine self-administration and extinction. **(A)** Self-administration and extinction of rats used for Western blotting and GFAP immunohistochemistry. **(B)** Western blotting for GFAP in the NAc core S2 subcellular fraction. GFAP signal was normalized to glyceraldehyde 3-phosphate dehydrogenase (GAPDH) loading control and converted to percent of the saline-administering control group. Western blot analysis revealed a significant decrease in signal following cocaine exposure in the NAc core, while no difference was observed in the prefrontal cortex (PFC). PFC tissue was taken from the dorsomedial prefrontal cortex, including prelimbic and anterior cingulate cortices. **(C, D)** Quantitative immunohistochemistry for GFAP was visualized using vasoactive intestinal peptide peroxidase substrate. Unbiased stereological counting was performed in the NAc core using MicroBrightField Stereoinvestigator. Estimated counts are reported as average (avg) of left and right hemisphere for each animal. These studies revealed fewer GFAP-positive astrocytes in the NAc core following self-administration and extinction. Representative images from saline (top) and cocaine-administering (bottom) animals are shown at $10\times$. $10\times$ scale bar = $100\ \mu\text{m}$. Inset at $40\times$. $*p < .05$ by Student unpaired two-tailed t test. ac, anterior commissure; C, cocaine; coc, cocaine; S, saline; sal, saline.

Accumbens Core Astrocytes Display Reduced Surface Area, Volume, and Colocalization With a Synaptic Marker Following Cocaine Self-Administration and Extinction

Similar to the astrocyte-enriched proteins GLT-1 and xCT (9), we observed decreased expression of GFAP in the NAc core following cocaine self-administration and extinction. However, GFAP represents a relatively minor fraction of overall astrocyte cell volume and is not localized in peripheral processes where neuronal and synaptic contact is made (26,27). To test the hypothesis that the downregulated GFAP is associated with quantifiable alterations in the morphology of astroglial cells, we transduced cells in the NAc core with an adeno-associated virus viral vector encoding a membrane-associated GFP (Lck-GFP) under the control of the GFAP promoter. Inclusion of the 11 amino acid Lck tag in the vector used to label astrocytes dramatically enhances the visualization of fine peripheral astrocytic processes by limiting expression of the fluorescent label to the plasma membrane (21,28). Viral infusion produced fields of transduced cells that displayed astroglial morphology throughout the NAc core (Figure 2; Supplemental Figure S1). Astrocytes with isolated margins were detectable and selected for analysis (Supplemental Figure S2).

In addition to labeling fine astroglial processes, GFP-expressing cells showed coregistry with GFAP in immunohistochemistry experiments (Supplemental Figure S1), indicating glial cell-type specific expression of the Lck-GFP.

Animals were trained to respond on a fixed-ratio 1 schedule of reinforcement for cocaine or saline in self-administration experiments. Following self-administration, responding was extinguished with repeated extinction training sessions where lever pressing did not result in the administration of cocaine or saline (Figure 3A). Twenty-four hours following the last extinction session, brain sections were prepared and imaged. Following image acquisition, deconvolution, and rendering of an intensity-based space-filling model for each astrocyte with the Imaris software, surface area and volume of 4 to 12 cells per animal were measured (Figure 3B, C). These analyses revealed a 19% decrease in volume (saline $31,242 \pm 1722\ \mu\text{m}^3$, cocaine $25,313 \pm 1110\ \mu\text{m}^3$; $t_{26} = 2.894$, $p = .008$) (Figure 1D) and a 21% decrease in surface area (saline $27,008 \pm 1035\ \mu\text{m}^2$, cocaine $23,279 \pm 1063\ \mu\text{m}^2$; $t_{26} = 2.513$, $p = .019$) following cocaine experience (Figure 3B).

Colocalization analyses of synaptic and astroglial GFP signals were performed using the Imaris software colocalization software toolkit as described previously (29) and

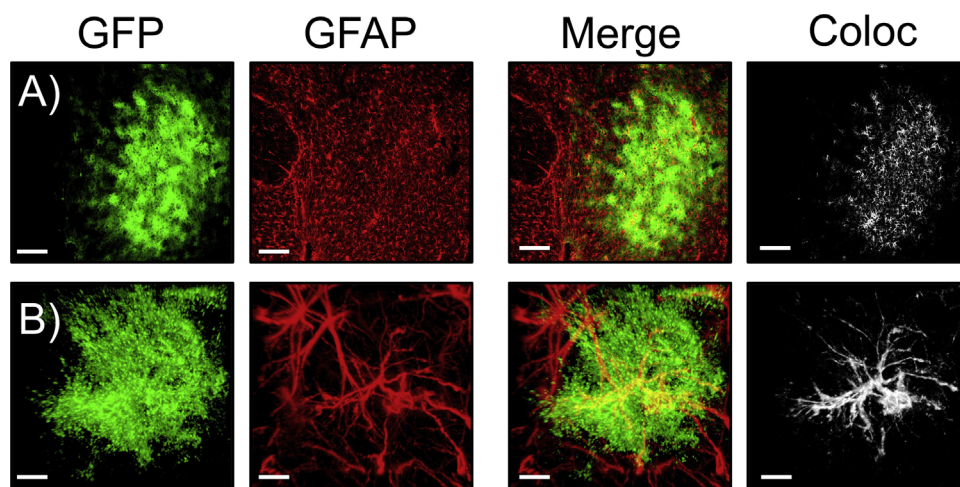


Figure 2. Adeno-associated virus type 5 GFAP-Lck-GFP drives membrane expression of GFP to nucleus accumbens (NAc) core astrocytes. **(A)** 10 \times images of Lck-GFP transduced NAc core astrocytes. Viral GFP expression is shown in green; GFAP immunohistochemistry is shown in red. The merged image (and the three-dimensional colocalization [Coloc] analysis performed in Imaris shown in white) demonstrates considerable coregistry of the GFP and GFAP signals, indicating astrocyte specific transduction. The white panel on far right shows voxels containing both viral GFP and GFAP immunohistochemistry signals. Scale bar = 150 μ m. **(B)** 63 \times z-series images of a single transduced astrocyte showing membrane-localized GFP expression in green, with GFAP immunohistochemistry in red.

chemistry in red. Both the merged image and white colocalization analysis show colocalization of the GFP and GFAP signals, again indicating astrocyte specific expression of GFP in the NAc core (see Supplemental Figure S1 for images from individual planes of the high-magnification z-series data set). Scale bar = 10 μ m. GFAP, glial fibrillary acidic protein; GFP, green fluorescent protein; Lck, lymphocyte protein tyrosine kinase.

consisted of an intensity-based measurement of the coregistry of Lck-GFP and synapsin voxels in a 3-D volume. It is important to note that the colocalization measured here does not indicate that synapsin is expressed or embedded in glial cells. Due to the close relationship between fine astroglial processes with neuronal processes (30), we interpret this measurement as an index of proximity by the astrocyte process and synapse. Our data demonstrate a significant decrease in

the coregistry of astroglial Lck-GFP and synapsin signals, observed as a 47% decrease in the percentage of voxels above threshold that contain both signals ($F_{2,30} = 4.678$, $p < .05$; Figure 4A, B, D). This value is defined by Imaris software as the percentage of region of interest colocalized (%ROI) (saline 0.10 ± 0.015 %ROI; cocaine 0.05 ± 0.007 %ROI) (Figure 4D). These data indicate that NAc core astrocytes make fewer proximal contacts with synapses following

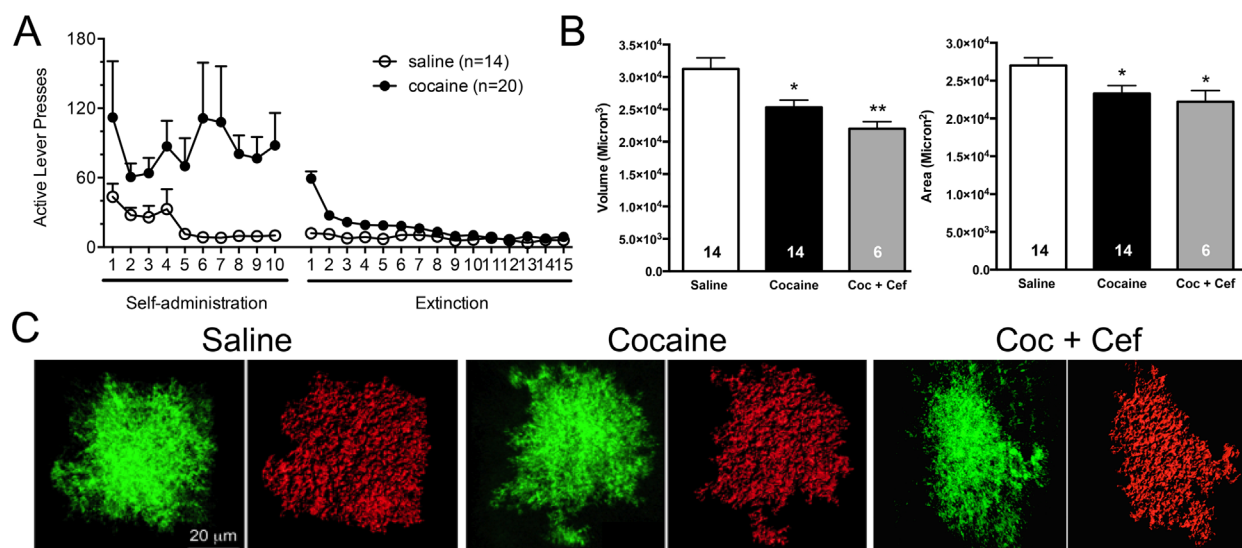


Figure 3. Three-dimensional (3-D) reconstruction of individual nucleus accumbens core astrocytes following cocaine (Coc) or saline experience. **(A)** Animals were trained to self-administer cocaine or saline and were then taken through extinction training. A subset of cocaine-administering rats received either saline or ceftriaxone (Cef) during extinction training. **(B)** Following rodent behavioral procedures, astrocyte green fluorescent protein (GFP) signals from adeno-associated virus type 5 GFAP-Lck-GFP transduced cells were used to generate 3-D space-filling models. Following deconvolution of z-series datasets, 3-D volumes generated by Imaris were constructed, which recapitulated the shape and contours of astroglial cells transduced with the membrane-localized GFP. Space-filling models were then used to determine surface area (μ m²) and volume (μ m³) of nucleus accumbens core astrocytes following cocaine or saline exposure. **(C)** Cocaine exposure significantly reduced astroglial volume as determined by analysis of Imaris space-filling astrocyte models (shown above in Figure 2). Two-tailed t tests revealed a significant reduction following cocaine exposure. Cocaine exposure also significantly reduced astroglial surface area. $p < .05$, $**p < .01$. GFAP, glial fibrillary acidic protein; Lck, lymphocyte protein tyrosine kinase.

cocaine exposure. Importantly, we observed no significant difference in the percentage of voxel intensities above threshold for either GFP (saline $43\% \pm 2.3\%$, cocaine $42.8\% \pm 1.7\%$) or synapsin (saline $35\% \pm 3.3\%$, cocaine $36\% \pm 1.7\%$) signals, indicating that a change in expression is unlikely to account for the observed change in colocalization.

Ceftriaxone Treatment Reverts Colocalization of Astroglial GFP and Synapsin Signals Marker to Saline Levels

To determine the impact of ceftriaxone treatment on astrocyte surface area, volume, and colocalization with synapsin, a subset of cocaine animals were treated with ceftriaxone or saline vehicle during the last 10 days of extinction training. Ceftriaxone has previously been shown to impair reinstatement to cocaine and restore numerous features of glutamate homeostasis in the NAc, including GLT-1 (9,20,31). Treatment with ceftriaxone did not revert cocaine-induced decreases in astrocyte volume (cocaine $25,313 \pm 1110 \mu\text{m}^3$, cocaine + ceftriaxone $22,027 \pm 1056 \mu\text{m}^3$; $t_{18} = 1.780$, $p = .092$) or surface area (cocaine $23,279 \pm 1063 \mu\text{m}^2$, cocaine + ceftriaxone $22,220 \pm 1473 \mu\text{m}^2$; $t_{18} = .5599$, $p = .5825$) in the NAc of cocaine-administering animals (Figure 3B, C); however, coregistry of Lck-GFP and synapsin voxels was reverted to saline levels following chronic ceftriaxone treatment during extinction

(saline $0.1\% \text{ROI}$ colocalized $\pm 0.015\%$, cocaine $0.05\% \text{ROI}$ colocalized $\pm 0.007\%$, and cocaine + ceftriaxone $0.1\% \text{ROI}$ colocalized $\pm 0.015\%$) (Figure 4D). The effect of ceftriaxone on astrocytes from saline-administering rats was not investigated, as previous studies have found ceftriaxone to be without effect on GLT-1 levels or extracellular glutamate levels in the NAc of saline-administering animals (9,20). There was no significant difference in the percentage of signal above threshold for either GFP (cocaine 42.85 ± 1.782 , saline 43 ± 2.310 , cocaine + ceftriaxone 38.67 ± 1.498) or synapsin (cocaine 35.77 ± 1.668 , saline 34.86 ± 3.259 , cocaine + ceftriaxone 36.33 ± 2.361) signals between groups.

DISCUSSION

Findings presented herein indicate a significant reduction in astrocyte volume and surface area as well as a significant decrease in the colocalization of astroglial processes with synapsin I in the NAc core following cocaine self-administration and extinction. Consistent with these findings, we observed downregulation of a primary astrocyte-specific structural filament protein GFAP, which is also in agreement with the altered morphometric properties of fluorescently labeled astrocytes. Interestingly, the cocaine-dependent decrease in synaptic contacts made by astrocytes was reversed by chronic treatment with ceftriaxone during extinction

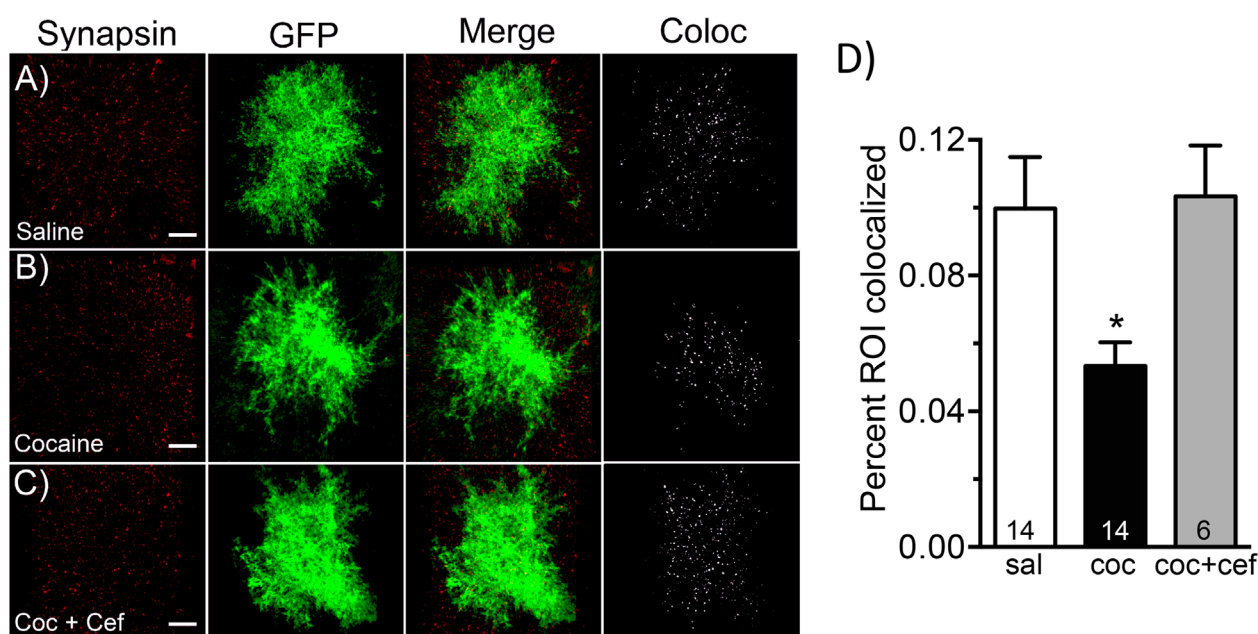


Figure 4. Three-dimensional colocalization (Coloc) analysis of synapsin I with astroglial membrane localized green fluorescent protein (GFP) in nucleus accumbens core astrocytes following cocaine (Coc) exposure. Brain tissue from animals transduced with the adeno-associated virus type 5 GFAP-Lck-GFP virus following saline (sal) or cocaine self-administration were stained with the synaptic marker synapsin. Following immunohistochemistry, individual astrocytes were imaged for both viral GFP expression and synapsin. Using Imaris, levels of colocalization (Coloc) between synapsin and GFP were assessed using the colocalization toolkit. **(A)** Viral GFP is shown in green for saline-administering animals along with synapsin I in red, a merged image as well as the colocalization channel, where voxels that contain both signals are shown in white. **(B)** This panel shows the same conditions described in **(A)** in animals following cocaine self-administration and extinction training. **(C)** Same conditions described in **(A)** in animals following cocaine self-administration and extinction training with ceftriaxone (Cef) treatment. **(D)** Using the Imaris colocalization toolkit, the percentage of the region of interest (ROI) colocalized was calculated for the astroglial membrane-specific GFP and synapsin signals for 4 to 12 cells per animal. Cocaine self-administration and extinction training significantly decreased the amount of colocalization of astroglial GFP with synapsin, which is reversed by administration of ceftriaxone during extinction training. * $p < .05$. GFAP, glial fibrillary acidic protein; Lck, lymphocyte protein tyrosine kinase.

tion training. Ceftriaxone has previously been shown to impair cocaine reinstatement by restoring measures of glutamate homeostasis in the NAc, an effect mediated largely by its ability to reverse cocaine-induced downregulation of GLT-1 (9,20,31,32). It is interesting to note that GLT-1 expression is specifically targeted to areas where astrocyte processes are closest to synapses (33) to provide efficient glutamate clearance and minimize spillover of synaptically released glutamate. Moreover, invasion of astroglial processes toward synapses is correlated with magnitude of GLT-1-mediated currents in astrocytes (34). Therefore, the previously reported capacity of ceftriaxone to restore expression of GLT-1 in cocaine-treated subjects (9,31), combined with our finding that ceftriaxone restores the synaptic localization of astroglial processes, argues that ceftriaxone facilitates glutamate uptake by positioning of astroglial processes containing GLT-1 to glutamate synapses. Taken together, our findings indicate that while withdrawal from noncontingent administration of both psychostimulants and opiates leads to evidence of reactive astrocytes characterized by increased GFAP (13,16), contingent cocaine self-administration and extinction leads to decreased GFAP expression, astrocyte shrinkage, and decreased association with synaptic elements. We hypothesize that differences in the regulation of GFAP expression in contingent versus noncontingent models likely arise due to different pharmacokinetic profiles of repeated single large doses of experimenter-administered drug versus the rate of administration achieved by the animal's control. However, it has been reported that while morphometric features of astrocytes, including overall size and complexity, are upregulated in the mouse dentate gyrus 24 hours after one noncontingent administration of cocaine, they are significantly decreased 24 hours following 7 or 14 days of administration (35).

It will be interesting to determine whether the changes observed following self-administration and extinction are also observed immediately following the self-administration stage or are also observed following forced abstinence in lieu of extinction training. The use of extinction in the reinstatement model of drug abuse allows for investigation of enduring cellular changes that contribute to mechanisms of reinstated drug seeking and has yielded a large body of literature on the cell biology of drug-seeking behavior (36). Salience of conditioned cues has been well described in human addicts (37); however, extinction training has yielded marginal success toward long-lasting relapse prevention, perhaps due, in part, to the complex nature of conditioned cues in an uncontrolled environment. Hence, more detailed investigation of the behavioral conditions in which cocaine-dependent adaptations to astrocytes are observed will inform the mechanism responsible for the observed changes.

Evidence for Hyporeactive Astrocytes in Psychiatric Disease

In cases of injury or inflammation in the brain, decreased GLT-1 expression is often associated with reactive astrocytes and increased GFAP expression (10–12,19). However, accumulating evidence indicates that in cases of psychiatric disease, specifically anxiety, stress, or depression, decreased GLT-1 expression coincides with decreased GFAP expression.

For example, GFAP messenger RNA is downregulated in both the cortex and hippocampus following chronic, but not acute, corticosterone treatment, while the astrocyte marker ALDH1L1 is unchanged (38). Chronic restraint stress results in decreased GFAP, as well as GLT-1 expression, in the periaqueductal gray (39), and loss of GFAP immunoreactivity, as well as astroglial GLT-1 expression, has been observed in the prefrontal cortex (40,41) and hypothalamus (42) in animal models of depression. Further, reductions in expression of GFAP have been reported in both preclinical animal models of depression and human postmortem studies of psychiatric disease, most notably depression but also schizophrenia [for review, see (43–45)]. Indeed, considerable evidence from the human literature indicates that glial dysfunction and more specifically decreased astrocyte density and astrocyte-mediated glutamate uptake may reflect a cellular feature of the high degree of comorbidity observed between substance use disorders and depression (46).

Experience-Dependent Adaptations in Synaptic Localization of Astrocyte Processes

A similar astroglial adaptation is observed in the supraoptic nucleus of the hypothalamus during lactation or dehydration [for review, see (47,48)]. In this case, reduced synaptic and somatic coverage by astrocytes results in impaired glutamate uptake, as well as impaired long-term potentiation and long-term depression (49), which closely parallels the capacity of cocaine treatment to simultaneously impair NAc core glutamate uptake and both long-term potentiation and long-term depression (50,51). As such, the disruption of astroglial morphology and synaptic contact may directly inhibit the ability to induce plasticity and represents a novel aspect of the drug-induced alterations in NAc core linked to relapse vulnerability.

Astrocytes closely interdigitate with neuronal processes at the level of individual dendritic spines (52), and there is strong evidence for cocaine-induced enhancement of dendritic spine density and head diameter in the NAc core (53–55). Given the reduction in astrocytic processes adjacent to synapses, we propose that cocaine experience causes NAc core astrocytes to move away from synapses, perhaps in part to make room in the neural parenchyma for new spines and the expansion of existing spine heads. Interestingly, while ceftriaxone normalizes glutamate homeostasis, GLT-1 expression, and synaptic colocalization of astrocyte processes, it is without effect on astrocyte volume or surface area, indicating that these adaptations may be mechanistically distinct. Previous studies indicate that GLT-1 expression and surface diffusion in the membrane is controlled by extracellular glutamate and neuronal activity (33,56). Thus, a priority of investigation is to functionally link these phenomena in the accumbens core with behavioral output (i.e., drug seeking).

ACKNOWLEDGMENTS AND DISCLOSURES

This work was supported by National Institutes of Health Grant Nos. R00DA031790 (to KJR), T32-DA007244 (to KLH), T32-DA007288 (to MDS), and R015369 and DA003906 (to PWK).

We thank Dr. Baljit Khakh for the kind gift of Lck-GFP plasmid.

The authors report no biomedical financial interests or potential conflicts of interest.

ARTICLE INFORMATION

From the Department of Neurosciences (MDS, HL, BS, PKT, HAB, PWK), Medical University of South Carolina, Charleston, South Carolina; and Department of Psychology and Neuroscience (KLH, NW, KJR) and Neuroscience Center (KJR), University of North Carolina at Chapel Hill, Chapel Hill, North Carolina.

HL and BS contributed equally to this work.

Address correspondence to Kathryn J. Reissner, Ph.D., University of North Carolina at Chapel Hill, Psychology and Neuroscience, 235 E Cameron Ave, Chapel Hill, NC 27599; E-mail: reissner@unc.edu.

Received Aug 17, 2015; revised Dec 2, 2015; accepted Dec 17, 2015.

Supplementary material cited in this article is available online at <http://dx.doi.org/10.1016/j.biopsych.2015.12.022>.

REFERENCES

- Allen NJ, Barres BA (2009): Neuroscience: Glia - more than just brain glue. *Nature* 457:675–677.
- Frank MG (2013): Astroglial regulation of sleep homeostasis. *Curr Opin Neurobiol* 23:812–818.
- Parpura V, Heneka MT, Montana V, Oliet SH, Schousboe A, Haydon PG, *et al.* (2012): Glial cells in (patho)physiology. *J Neurochem* 121:4–27.
- Verkhratsky A, Parpura V (2016): Astroglipathology in neurological, neurodevelopmental and psychiatric disorders. *Neurobiol Dis* 85:254–261.
- Bull C, Syed WA, Minter SC, Bowers MS (2015): Differential response of glial fibrillary acidic protein-positive astrocytes in the rat prefrontal cortex following ethanol self-administration. *Alcohol Clin Exp Res* 39:650–658.
- Scofield MD, Boger HA, Smith RJ, Li H, Haydon PG, Kalivas PW (2015): Gq-DREADD selectively initiates glial glutamate release and inhibits cue-induced cocaine seeking. *Biol Psychiatry* 78:441–451.
- Turner JR, Ecker LE, Briand LA, Haydon PG, Blendy JA (2013): Cocaine-related behaviors in mice with deficient gliotransmission. *Psychopharmacology (Berl)* 226:167–176.
- Scofield MD, Kalivas PW (2014): Astrocytic dysfunction and addiction: Consequences of impaired glutamate homeostasis. *Neuroscientist* 20:610–622.
- Knackstedt LA, Melendez RI, Kalivas PW (2010): Ceftriaxone restores glutamate homeostasis and prevents relapse to cocaine seeking. *Biol Psychiatry* 67:81–84.
- Hamby ME, Sofroniew MV (2010): Reactive astrocytes as therapeutic targets for CNS disorders. *Neurotherapeutics* 7:494–506.
- Yi JH, Hazell AS (2006): Excitotoxic mechanisms and the role of astrocytic glutamate transporters in traumatic brain injury. *Neurochem Int* 48:394–403.
- Colangelo AM, Alberghina L, Papa M (2014): Astroglialosis as a therapeutic target for neurodegenerative diseases. *Neurosci Lett* 565:59–64.
- Bowers MS, Kalivas PW (2003): Forebrain astroglial plasticity is induced following withdrawal from repeated cocaine administration. *Eur J Neurosci* 17:1273–1278.
- Narita M, Suzuki M, Kuzumaki N, Miyatake M, Suzuki T (2008): Implication of activated astrocytes in the development of drug dependence: Differences between methamphetamine and morphine. *Ann N Y Acad Sci* 1141:96–104.
- Cooper ZD, Jones JD, Comer SD (2012): Glial modulators: A novel pharmacological approach to altering the behavioral effects of abused substances. *Expert Opin Investig Drugs* 21:169–178.
- Clark KH, Wiley CA, Bradberry CW (2013): Psychostimulant abuse and neuroinflammation: Emerging evidence of their interconnection. *Neurotox Res* 23:174–188.
- Watkins LR, Hutchinson MR, Milligan ED, Maier SF (2007): “Listening” and “talking” to neurons: Implications of immune activation for pain control and increasing the efficacy of opioids. *Brain Res Rev* 56:148–169.
- Loftis JM, Janowsky A (2014): Neuroimmune basis of methamphetamine toxicity. *Int Rev Neurobiol* 118:165–197.
- Anderson MA, Ao Y, Sofroniew MV (2014): Heterogeneity of reactive astrocytes. *Neurosci Lett* 565:23–29.
- Trantham-Davidson H, LaLumiere RT, Reissner KJ, Kalivas PW, Knackstedt LA (2012): Ceftriaxone normalizes nucleus accumbens synaptic transmission, glutamate transport, and export following cocaine self-administration and extinction training. *J Neurosci* 32:12406–12410.
- Shigetomi E, Bushong EA, Haustein MD, Tong X, Jackson-Weaver O, Kracun S, *et al.* (2013): Imaging calcium microdomains within entire astrocyte territories and endfeet with GCaMPs expressed using adeno-associated viruses. *J Gen Physiol* 141:633–647.
- Paxinos G, Watson C (2007): *The Rat Brain in Stereotaxic Coordinates, 6th ed.* Burlington, VT: Elsevier Academic Press.
- Gundersen HJ, Jensen EB (1987): The efficiency of systematic sampling in stereology and its prediction. *J Microsc* 147:229–263.
- Boger HA, Middaugh LD, Huang P, Zaman V, Smith AC, Hoffer BJ, *et al.* (2006): A partial GDNF depletion leads to earlier age-related deterioration of motor function and tyrosine hydroxylase expression in the substantia nigra. *Exp Neurol* 202:336–347.
- Landmann L (2002): Deconvolution improves colocalization analysis of multiple fluorochromes in 3D confocal data sets more than filtering techniques. *J Microsc* 208:134–147.
- Sofroniew MV, Vinters HV (2010): Astrocytes: Biology and pathology. *Acta Neuropathol* 119:7–35.
- Oberheim NA, Takano T, Han X, He W, Lin JH, Wang F, *et al.* (2009): Uniquely hominid features of adult human astrocytes. *J Neurosci* 29:3276–3287.
- Benediktsson AM, Schachtele SJ, Green SH, Dailey ME (2005): Ballistic labeling and dynamic imaging of astrocytes in organotypic hippocampal slice cultures. *J Neurosci Methods* 141:41–53.
- Kupchik YM, Brown RM, Heinsbroek JA, Lobo MK, Schwartz DJ, Kalivas PW (2015): Coding the direct/indirect pathways by D1 and D2 receptors is not valid for accumbens projections. *Nat Neurosci* 18:1230–1232.
- Ventura R, Harris KM (1999): Three-dimensional relationships between hippocampal synapses and astrocytes. *J Neurosci* 19:6897–6906.
- Sari Y, Smith KD, Ali PK, Rebec GV (2009): Upregulation of GLT1 attenuates cue-induced reinstatement of cocaine-seeking behavior in rats. *J Neurosci* 29:9239–9243.
- Sondheimer I, Knackstedt LA (2011): Ceftriaxone prevents the induction of cocaine sensitization and produces enduring attenuation of cue- and cocaine-primed reinstatement of cocaine-seeking. *Behav Brain Res* 225:252–258.
- Yang Y, Gozen O, Watkins A, Lorenzini I, Lepore A, Gao Y, *et al.* (2009): Presynaptic regulation of astroglial excitatory neurotransmitter transporter GLT1. *Neuron* 61:880–894.
- Pannasch U, Freche D, Dallerac G, Ghezali G, Escartin C, Ezan P, *et al.* (2014): Connexin 30 sets synaptic strength by controlling astroglial synapse invasion. *Nat Neurosci* 17:549–558.
- Fattore L, Puddu MC, Picciau S, Cappai A, Fratta W, Serra GP, *et al.* (2002): Astroglial in vivo response to cocaine in mouse dentate gyrus: A quantitative and qualitative analysis by confocal microscopy. *Neuroscience* 110:1–6.
- Bossert JM, Marchant NJ, Calu DJ, Shaham Y (2013): The reinstatement model of drug relapse: Recent neurobiological findings, emerging research topics, and translational research. *Psychopharmacology (Berl)* 229:453–476.
- Peck JA, Ranaldi R (2014): Drug abstinence: Exploring animal models and behavioral treatment strategies. *Psychopharmacology* 231:2045–2058.
- Carter BS, Hamilton DE, Thompson RC (2013): Acute and chronic glucocorticoid treatments regulate astrocyte-enriched mRNAs in multiple brain regions in vivo. *Front Neurosci* 7:139.
- Imbe H, Kimura A, Donishi T, Kaneoke Y (2012): Chronic restraint stress decreases glial fibrillary acidic protein and glutamate transporter in the periaqueductal gray matter. *Neuroscience* 223:209–218.

40. Banasr M, Duman RS (2008): Glial loss in the prefrontal cortex is sufficient to induce depressive-like behaviors. *Biol Psychiatry* 64:863–870.
41. Banasr M, Chowdhury GM, Terwilliger R, Newton SS, Duman RS, Behar KL, Sanacora G (2010): Glial pathology in an animal model of depression: Reversal of stress-induced cellular, metabolic and behavioral deficits by the glutamate-modulating drug riluzole. *Mol Psychiatry* 15:501–511.
42. Gunn BG, Cunningham L, Cooper MA, Corteen NL, Seifi M, Swinny JD, *et al.* (2013): Dysfunctional astrocytic and synaptic regulation of hypothalamic glutamatergic transmission in a mouse model of early-life adversity: Relevance to neurosteroids and programming of the stress response. *J Neurosci* 33:19534–19554.
43. Banasr M, Dwyer JM, Duman RS (2011): Cell atrophy and loss in depression: Reversal by antidepressant treatment. *Curr Opin Cell Biol* 23:730–737.
44. Cotter DR, Pariante CM, Everall IP (2001): Glial cell abnormalities in major psychiatric disorders: The evidence and implications. *Brain Res Bull* 55:585–595.
45. Molofsky AV, Krencik R, Ullian EM, Tsai HH, Deneen B, Richardson WD, *et al.* (2012): Astrocytes and disease: A neurodevelopmental perspective. *Genes Dev* 26:891–907.
46. Niciu MJ, Henter ID, Sanacora G, Zarate CA Jr (2014): Glial abnormalities in substance use disorders and depression: Does shared glutamatergic dysfunction contribute to comorbidity? *World J Biol Psychiatry* 15:2–16.
47. Piet R, Poulain DA, Oliet SH (2004): Contribution of astrocytes to synaptic transmission in the rat supraoptic nucleus. *Neurochem Int* 45:251–257.
48. Theodosis DT, Poulain DA (1993): Activity-dependent neuronal-glial and synaptic plasticity in the adult mammalian hypothalamus. *Neuroscience* 57:501–535.
49. Panatier A, Theodosis DT, Mothet JP, Touquet B, Pollegioni L, Poulain DA, Oliet SH (2006): Glia-derived D-serine controls NMDA receptor activity and synaptic memory. *Cell* 125:775–784.
50. Moussawi K, Pacchioni A, Moran M, Olive MF, Gass JT, Lavin A, Kalivas PW (2009): N-Acetylcysteine reverses cocaine-induced meta-plasticity. *Nat Neurosci* 12:182–189.
51. Martin M, Chen BT, Hopf FW, Bowers MS, Bonci A (2006): Cocaine self-administration selectively abolishes LTD in the core of the nucleus accumbens. *Nat Neurosci* 9:868–869.
52. Witcher MR, Ellis TL (2012): Astroglial networks and implications for therapeutic neuromodulation of epilepsy. *Front Comput Neurosci* 6:61.
53. Norrholm SD, Bibb JA, Nestler EJ, Ouimet CC, Taylor JR, Greengard P (2003): Cocaine-induced proliferation of dendritic spines in nucleus accumbens is dependent on the activity of cyclin-dependent kinase-5. *Neuroscience* 116:19–22.
54. Shen HW, Toda S, Moussawi K, Bouknight A, Zahm DS, Kalivas PW (2009): Altered dendritic spine plasticity in cocaine-withdrawn rats. *J Neurosci* 29:2876–2884.
55. Stefanik MT, Kupchik YM, Kalivas PW (2015): Optogenetic inhibition of cortical afferents in the nucleus accumbens simultaneously prevents cue-induced transient synaptic potentiation and cocaine-seeking behavior [published online ahead of print February 7]. *Brain Struct Funct*.
56. Murphy-Royal C, Dupuis JP, Varela JA, Panatier A, Pinson B, Baufreton J, *et al.* (2015): Surface diffusion of astrocytic glutamate transporters shapes synaptic transmission. *Nat Neurosci* 18: 219–226.